Thermal buckling of functionally graded sandwich plates using a new hyperbolic shear displacement model

Fatima Zohra Kettaf [1], Mohammed Sid Ahmed Houari [2],
Mohamed Benguediab [1] and Abdelouahed Tounsi[*2,3,4]

[1] *Département de Génie Mécanique, Faculté de Technologie, Université Sidi Bel Abbes, Algérie*
[2] *Laboratoire des Structures et Matériaux Avancés dans le Génie Civil et Travaux Publics,*
Université de Sidi Bel Abbes, Faculté de Technologie, BP 89 Cité Ben M'hidi 22000 Sidi Bel Abbes, Algérie
[3] *Laboratoire des Matériaux et Hydrologie, Université de Sidi Bel Abbes, Faculté de Technologie,*
BP 89 Cité Ben M'hidi 22000 Sidi Bel Abbes, Algérie
[4] *Département de Génie Civil, Faculté de Technologie, Université Sidi Bel Abbes, Algérie*

Abstract. In the present study, the thermal buckling behavior of functionally graded sandwich plates is studied using a new hyperbolic displacement model. Unlike any other theory, the theory is variationally consistent and gives four governing equations. Number of unknown functions involved in displacement field is only four, as against five in case of other shear deformation theories. This present model takes into account the parabolic distribution of transverse shear stresses and satisfies the condition of zero shear stresses on the top and bottom surfaces without using shear correction factor. Material properties and thermal expansion coefficient of the sandwich plate faces are assumed to be graded in the thickness direction according to a simple power-law distribution in terms of the volume fractions of the constituents. The core layer is still homogeneous and made of an isotropic material. The thermal loads are assumed as uniform, linear and non-linear temperature rises across the thickness direction. The results reveal that the volume fraction index, loading type and functionally graded layers thickness have significant influence on the thermal buckling of functionally graded sandwich plates.

Keywords: new plate theory; thermal buckling; functionally graded plate; volume fraction index

1. Introduction

Functionally graded materials (FGMs) are microscopically inhomogeneous composites usually made of a mixture of metals and ceramics. By gradually varying the volume fraction of their constituents, it can be achieved that the effective properties of FGMs exhibit a smooth and continuous change from one surface to another, thus eliminating interface problems and mitigating thermal stress concentrations. Due to the high heat resistance, FGMs are used as structural components operating in ultrahigh-temperature environments and subjected to extremely high thermal gradients, such as aircraft, space vehicles, nuclear plants, and other engineering applications.

∗Corresponding author, Professor, E-mail: tou_abdel@yahoo.com

The functionally graded (FG) plates are commonly used in thermal environments; they can buckle under thermal and mechanical loads. Thus, the buckling analysis of such plates is essential to ensure an efficient and reliable design. The classical plate theory (CPT) is usually used to carry out stability analysis of thin FG plates (Javaheri and Eslami 2002a). This theory ignores the transverse shear deformation and assumes that the normal to the middle plane before deformation remains straight and normal to the middle surface after deformation. As a result, the classical plate theory overestimates the buckling load except for truly thin plates. The first-order shear deformation theory (FSDT), including the effects of transverse shear deformation, was employed by some researches to analyze buckling behavior of moderately thick FG plates (Wu 2004, Samsam Shariat and Eslami 2005, Bouazza *et al*. 2010, Yaghoobi and Yaghoobi 2013). The FSDT assumes a constant value of transverse shear strain through the thickness of the plate and requires shear correction factor to correct for the discrepancy between the actual transverse shear strain and the constant one. The shear correction factor, which is crucial to an accurate analysis, depends on geometric parameters, loadings, material and boundary conditions of the plate. Also in the FSDT, the cross-sectional warping is neglected as it is assumed that the plane sections remain plane. According to the viewpoint of some research groups, the first-order shear deformation theory is not a proper model for analyzing thick structures (Reddy 1984, 2000, Javaheri and Eslami 2002b, Şimşek 2009, Sallai *et al*. 2009). To overcome the drawbacks of these theories (i.e., CPT and FSDT), various higher-order plate theories have been proposed by assuming higher-order displacement fields. Among these theories, the higher-order shear deformation theory (HSDT) of Reddy (1984) has been extensively used for analysis of thick plates. The HSDT assumes third-order polynomials in the expansion of the displacement components through the thickness and accommodates a parabolic variation of the transverse shear strains and stresses through the thickness and the vanishing of transverse shear stresses on the top and bottom surfaces of the plate. Unlike the FSDT, the HSDT requires no shear correction factor and also the cross-sections of plate are allowed to warp.

To the best of authors' knowledge, there are a little research works for thermal buckling analysis of functionally graded rectangular plates based on higher-order shear deformation theories in the open literature. Javaheri and Eslami (2002b) studied thermal buckling of simply supported FG plates subjected to various types of thermal loadings based on the higher-order shear deformation theory. They presented the buckling temperatures in closed-form solutions using Navier's method. Samsam Shariat and Eslami (2007) presented the mechanical and thermal buckling analysis of thick functionally graded rectangular plates. They used the third-order shear deformation plate theory and Navier's method to obtain the closed-form solutions for the critical buckling load and temperature of a simply supported rectangular plate whose material properties vary linearly with respect to the thickness coordinate. Using the method of power series expansion of displacement components, Matsunaga (2009) presented a higher order deformation theory for thermal buckling of functionally graded rectangular plates. However, there are a few reported studies on the thermal buckling analysis of FG sandwich plates. Liew *et al*. (2004) discussed the post-buckling and buckling of moderately thick composite plates comprising FG layers under thermal loading. Both perfect and imperfect FG plates are considered, and temperature dependency of material constituents is also included. Na and Kim (2006) presented a finite element formulation to predict the instability of clamped unsymmetric composite FG plates. In their study, temperature dependency of material properties is also included. Recently, Zenkour and Sobhy (2010) studied the thermal buckling of functionally graded sandwich plates using sinusoidal shear deformation plate theory. A simple approximate closed-form expression to predict the

thermal post-buckling response of sandwich plates with FGM face sheets is presented by Kiani and Eslami (2012) with considering the temperature dependency of thermomechanical properties.

Although some studies have been carried out for the thermal buckling analysis of FG plates by using higher-order shear deformation theories with five unknown functions, no studies can be found for the thermal buckling analysis of functionally graded rectangular plates with new class of plate theories such as the four variable refined plate theory. Thus, the purpose of this paper is to study the critical buckling temperature for symmetric FG sandwich plates using a four variable refined plate theory. Tounsi and his associates recently developed this new plate theory (Houari *et al*. 2011, Ameur *et al*. 2011, Merdaci *et al*. 2011, El Meiche *et al*. 2011, Bourada *et al*. 2012, Fekrar *et al*. 2012, Bouderba *et al*. 2013). This theory which looks like higher-order theory uses only four unknown functions in order to derive four governing equations for functionally graded plates. The most interesting feature of this theory is that it does not require shear correction factor, and accounts for parabolic distribution of the transverse shear strains, and satisfies the zero traction boundary conditions on the surfaces of the plate without using shear correction factor. The accuracy of this theory has been demonstrated for static and thermoelastic behavior of FG plates by Houari *et al*. (2011) and Merdaci *et al*. (2011). Ameur *et al*. (2011) presented a new trigonometric shear deformation plate theory involving only four unknown functions for flexural analysis of FG plates resting on an elastic foundation. El Meiche *et al*. (2011) studied the buckling and vibration of FG sandwich plates using a new refined hyperbolic shear deformable plate theory with only four unknown functions. In the present study, the four variable refined plate theories have been extended to the thermal buckling behavior of FG sandwich plates. For this end, a new hyperbolic displacement model is developed to deduce the stability equations. The material properties as Young's modulus and coefficient of thermal expansion vary according to a power law form through-the-thickness coordinate. The governing equations are solved analytically for a plate with simply-supported boundary conditions and subjected to various type of temperature rise. Then, an eigenvalue problem is formulated for a simply supported FG sandwich plate to analyze its thermal buckling behaviors. The effects of various variables, such as FG layer thickness, volume fraction index, thickness ratio, and aspect ratio, on the thermal buckling temperature of FG sandwich plate are investigated and discussed. An eigenvalue problem is formulated for a simply supported FGM sandwich plates to analyze its thermal buckling behaviors. The thermal loads are assumed as uniform, linear and non-linear temperature rises across the thickness direction. Illustrative examples are given so as to demonstrate the efficacies of the present model. The effects of various variables, such as thickness and aspect ratios, gradient index, loading type and sandwich plate type on the critical buckling are all discussed.

2. Modeling of functionally graded material

Consider a flat sandwich plate composed of three (metal-ceramic, ceramic, ceramic-metal) layers as shown in Fig. 1. Rectangular Cartesian coordinates (x, y, z) are used to describe infinitesimal deformations of a three-layer sandwich elastic plate occupying the region $[0, a] \times [0, b] \times [-h/2, h/2]$ in the unstressed reference configuration. The mid-plane is defined by $z = 0$ and its external bounding planes being defined by $z = \pm h/2$. The face layers of the sandwich plate are made of an isotropic material with material properties varying smoothly in the z (thickness) direction only. The core layer is made of an isotropic homogeneous material. The vertical positions of the bottom surface, the two interfaces between the core and faces layers, and the top
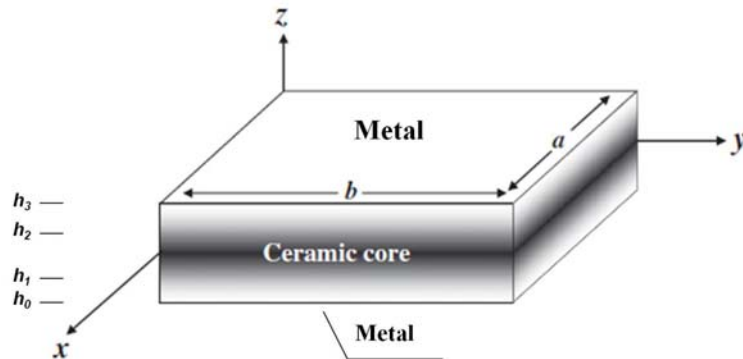
Fig. 1 Geometry of the FGM sandwich plate

surface are denoted, respectively, by $h_0 = -h/2$, h_1, h_2 and $h_3 = h/2$. The total thickness of the FG plate is h, where $h = t_C + t_{FGM}$ and $t_C = h_2 - h_1$. t_C and t_{FGM} are the layer thickness of the core and all-FGM layers, respectively.

The effective material properties for each layer, like Young's modulus, Poisson's ratio and thermal expansion coefficient, can be expressed as

$$P^{(n)}(z) = P_m + (P_c - P_m)V^{(n)} \tag{1}$$

where $P^{(n)}$ is the effective material property of FGM of layer n. P_m and P_c denote the property of the bottom and top faces of layer 1 ($h_0 \le z \le h_1$), respectively, and vice versa for layer 3 ($h_2 \le z \le h_3$) depending on the volume fraction $V^{(n)}$ ($n = 1, 2, 3$). Note that P_m and P_c are, respectively, the corresponding properties of the metal and ceramic of the FGM sandwich plate. The volume fraction $V^{(n)}$ of the FGMs is assumed to obey a power-law function along the thickness direction (Houari *et al.* 2011)

$$V^{(1)} = \left(\frac{z - h_0}{h_1 - h_0}\right)^k, \quad z \in [h_0, h_1] \tag{2a}$$

$$V^{(2)} = 1, \qquad z \in [h_1, h_2] \tag{2b}$$

$$V^{(3)} = \left(\frac{z - h_3}{h_2 - h_3}\right)^k, \quad z \in [h_2, h_3] \tag{2c}$$

where k is the volume fraction exponent, which takes values greater than or equals to zero. The core layer is independent of the value of k which is a fully ceramic layer. However, the value of k equal to zero represents a fully ceramic plate. The above power-law assumption given in Eqs. (2a) and (2c) reflects a simple rule of mixtures used to obtain the effective properties of the metal-ceramic and ceramic-metal plate faces (see Fig. 1). Fig. 2 shows the through-the-thickness variation of the volume fraction function of the ceramic for $k = 0.01, 0.2, 0.5, 2, 5$, and 10. Note that the core of the plate is fully ceramic while the bottom and top surfaces of the plate are metal-rich.
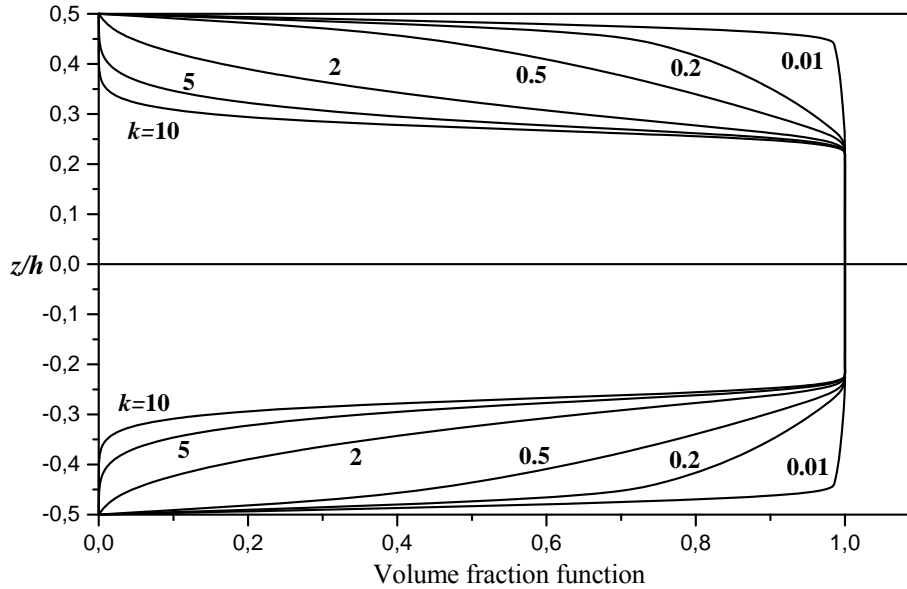
Fig. 2 Variation of volume fraction function through plate thickness for various values of the power-law index k with $t_C / h = 0.5$

2.1 Higher-order plate theories with five unknown functions

The displacements of a material point located at (x, y, z) in the plate may be written as

$$u = u_0(x, y) - z \frac{\partial w_0}{\partial x} + \Psi(z) \theta_x \tag{3a}$$

$$v = v_0(x, y) - z \frac{\partial w_0}{\partial y} + \Psi(z) \theta_y \tag{3b}$$

$$w = w_0(x, y) \tag{3c}$$

where, u, v, w are displacements in the x, y, z directions, u_0, v_0 and w_0 are midplane displacements, θ_x and θ_y rotations of the yz and xz planes due to bending, respectively. $\Psi(z)$ represents shape function determining the distribution of the transverse shear strains and stresses along the thickness. The displacement field of the classical thin plate theory (CPT) is obtained easily by setting $\Psi(z) = 0$. The displacement of the first-order shear deformation plate theory (FSDPT) is obtained by setting $\Psi(z) = z$. Also, the displacement of third-order shear deformation plate theory (TSDPT) of Reddy (1984) is obtained by setting

$$\Psi(z) = z \left(1 - \frac{4z^2}{3h^2} \right) \tag{4a}$$

The sinusoidal shear deformation plate theory (SSDPT) of Zenkour (2005) is obtained by

setting

$$\Psi(z) = \frac{h}{\pi} \sin\left(\frac{\pi z}{h}\right) \tag{4b}$$

2.2 Present new hyperbolic displacement model

The present theory has the following features
- It is a displacement-based theory which includes the transverse shear effects.
- Number of unknown functions involved in the theory is only four. Even in the Reissner's and Mindlin's theory (FSDPT), five unknown functions are involved.
- The theory is variationally consistent.
- Transverse shear stress satisfies zero shear stress boundary conditions on top and bottom surfaces of the beam perfectly.
- The theory obviates the need of shear correction factor

2.2.1 Assumptions of the new hyperbolic displacement model
Assumptions of the present theory are as follows
(i)   The displacements are small in comparison with the plate thickness and, therefore, strains involved are infinitesimal.
(ii) The transverse displacement w includes two components of bending w_b, and shear w_s. These components are functions of coordinates x, y only.

$$w(x, y, z) = w_b(x, y) + w_s(x, y) \tag{5}$$

(iii) The transverse normal stress σ_z is negligible in comparison with in-plane stresses σ_x and σ_y.
(iv) The displacements u in x-direction and v in y-direction consist of extension, bending, and shear components.

$$u = u_0 + u_b + u_s, \quad v = v_0 + v_b + v_s \tag{6}$$

The bending components u_b and v_b are assumed to be similar to the displacements given by the classical plate theory. Therefore, the expression for u_b and v_b can be given as

$$u_b = -z\frac{\partial w_b}{\partial x}, \quad v_b = -z\frac{\partial w_b}{\partial y} \tag{7}$$

The shear components u_s and v_s give rise, in conjunction with w_s, to the parabolic variations of shear strains γ_{xz}, γ_{yz} and hence to shear stresses τ_{xz}, τ_{yz} through the thickness of the plate in such a way that shear stresses τ_{xz}, τ_{yz} are zero at the top and bottom faces of the plate. Consequently, the expression for u_s and v_s can be given as

$$u_s = -f(z)\frac{\partial w_s}{\partial x}, \quad v_s = -f(z)\frac{\partial w_s}{\partial y} \tag{8}$$

2.2.2 Kinematics and constitutive equations

Based on the assumptions made in the preceding section, the displacement field can be obtained using Eqs. (5)-(8) as

$$u(x,y,z) = u_0(x,y) - z\frac{\partial w_b}{\partial x} - f(z)\frac{\partial w_s}{\partial x}$$

$$v(x,y,z) = v_0(x,y) - z\frac{\partial w_b}{\partial y} - f(z)\frac{\partial w_s}{\partial y} \qquad (9a)$$

$$w(x,y,z) = w_b(x,y) + w_s(x,y)$$

The function $f(z)$ is chosen in the form

$$f(z) = z\left[1 + \frac{3\pi}{2}\sec h^2\left(\frac{1}{2}\right)\right] - \frac{3\pi}{2}h\tanh\left(\frac{z}{h}\right) \qquad (9b)$$

The non-linear von Karman strain–displacement equations are as follows

$$\varepsilon_x = \frac{\partial u}{\partial x} + \frac{1}{2}\left(\frac{\partial w_b}{\partial x} + \frac{\partial w_s}{\partial x}\right)^2,$$

$$\varepsilon_y = \frac{\partial v}{\partial y} + \frac{1}{2}\left(\frac{\partial w_b}{\partial y} + \frac{\partial w_s}{\partial y}\right)^2,$$

$$\varepsilon_z = \frac{\partial w_b}{\partial z} + \frac{\partial w_s}{\partial z} = 0,$$

$$\gamma_{xy} = \frac{\partial v}{\partial x} + \frac{\partial u}{\partial y} + \left(\frac{\partial w_b}{\partial x} + \frac{\partial w_s}{\partial x}\right)\left(\frac{\partial w_b}{\partial y} + \frac{\partial w_s}{\partial y}\right), \qquad (10)$$

$$\gamma_{yz} = \frac{\partial v}{\partial z} + \left(\frac{\partial w_b}{\partial y} + \frac{\partial w_s}{\partial y}\right),$$

$$\gamma_{xz} = \frac{\partial u}{\partial z} + \left(\frac{\partial w_b}{\partial x} + \frac{\partial w_s}{\partial x}\right),$$

On the basis of the displacement field given in Eq. (9), Eq. (10) becomes

$$\varepsilon_x = \varepsilon_x^0 + z\,k_x^b + f(z)\,k_x^s$$

$$\varepsilon_y = \varepsilon_y^0 + z\,k_y^b + f(z)\,k_y^s$$

$$\gamma_{xy} = \gamma_{xy}^0 + z\,k_{xy}^b + f(z)\,k_{xy}^s$$

$$\gamma_{yz} = g(z)\,\gamma_{yz}^s \qquad (11)$$

$$\gamma_{xz} = g(z)\,\gamma_{xz}^s$$

$$\varepsilon_z = 0$$

where

$$\varepsilon_x^0 = \frac{\partial u_0}{\partial x} + \frac{1}{2}\left(\frac{\partial w_b}{\partial x} + \frac{\partial w_s}{\partial x}\right)^2, \qquad k_x^b = -\frac{\partial^2 w_b}{\partial x^2}, \qquad k_x^s = -\frac{\partial^2 w_s}{\partial x^2}$$

$$\varepsilon_y^0 = \frac{\partial v_0}{\partial y} + \frac{1}{2}\left(\frac{\partial w_b}{\partial y} + \frac{\partial w_s}{\partial y}\right), \qquad k_y^b = -\frac{\partial^2 w_b}{\partial y^2}, \qquad k_y^s = -\frac{\partial^2 w_s}{\partial y^2}$$

$$\gamma_{xy}^0 = \frac{\partial v_0}{\partial x} + \frac{\partial u_0}{\partial y} + \left(\frac{\partial w_b}{\partial x} + \frac{\partial w_s}{\partial x}\right)\left(\frac{\partial w_b}{\partial y} + \frac{\partial w_s}{\partial y}\right), \quad k_{xy}^b = -2\frac{\partial^2 w_b}{\partial x \partial y}, \qquad k_{xy}^s = -2\frac{\partial^2 w_s}{\partial x \partial y} \tag{12}$$

$$\gamma_{yz}^s = \frac{\partial w_s}{\partial y}, \qquad \gamma_{xz}^s = \frac{\partial w_s}{\partial x}, \qquad g(z) = 1 - f'(z) \quad \text{and} \quad f'(z) = \frac{df(z)}{dz}$$

For elastic and isotropic FGMs, the constitutive relations can be written as

$$\begin{Bmatrix} \sigma_x \\ \sigma_y \\ \tau_{xy} \end{Bmatrix}^{(n)} = \begin{bmatrix} Q_{11} & Q_{12} & 0 \\ Q_{12} & Q_{22} & 0 \\ 0 & 0 & Q_{66} \end{bmatrix}^{(n)} \begin{Bmatrix} \varepsilon_x - \alpha T \\ \varepsilon_y - \alpha T \\ \gamma_{xy} \end{Bmatrix}^{(n)} \quad \text{and} \quad \begin{Bmatrix} \tau_{yz} \\ \tau_{zx} \end{Bmatrix}^{(n)} = \begin{bmatrix} Q_{44} & 0 \\ 0 & Q_{55} \end{bmatrix}^{(n)} \begin{Bmatrix} \gamma_{yz} \\ \gamma_{zx} \end{Bmatrix}^{(n)} \tag{13}$$

where (σ_x, σ_y, τ_{xz}, τ_{yz}, τ_{yx}) and (ε_x, ε_y, γ_{xy}, γ_{yz}, γ_{yx}) are the stress and strain components, respectively. Using the material properties defined in Eq. (1), stiffness coefficients, Q_{ij}, can be expressed as

$$Q_{11}^{(n)} = Q_{22}^{(n)} = \frac{E^{(n)}(z)}{1 - v^2}, \tag{14a}$$

$$Q_{12}^{(n)} = \frac{v\,E^{(n)}(z)}{1 - v^2}, \tag{14b}$$

$$Q_{44}^{(n)} = Q_{55}^{(n)} = Q_{66}^{(n)} = \frac{E^{(n)}(z)}{2(1 + v)}, \tag{14c}$$

and $T(x, y, z)$ is the temperature rise through-the-thickness.

2.3 Stability equations

The total potential energy of the FGM sandwich plate may be written as

$$U = \frac{1}{2}\iiint \left[\sigma_x^{(n)}\left(\varepsilon_x - \alpha^{(n)}T\right) + \sigma_y^{(n)}\left(\varepsilon_y - \alpha^{(n)}T\right) + \tau_{xy}^{(n)}\gamma_{xy} + \tau_{yz}^{(n)}\gamma_{yz} + \tau_{xz}\gamma_{xz}\right]dxdydz, \tag{15}$$

The principle of virtual work for the present problem may be expressed as follows

$$\iint \left[N_x \delta\,\varepsilon_x^0 + N_y \delta\,\varepsilon_y^0 + N_{xy}\delta\,\gamma_{xy}^0 + M_x^b \delta\,k_x^b + M_y^b \delta\,k_y^b + M_{xy}^b \delta\,k_{xy}^b \right.$$
$$\left. + M_x^s \delta\,k_x^s + M_y^s \delta\,k_y^s + M_{xy}^s \delta\,k_{xy}^s + S_{yz}^s \delta\,\gamma_{yz}^s + S_{xz}^s \delta\,\gamma_{xz}^s \right]dxdy = 0 \tag{16}$$

where

$$
\left\{
\begin{array}{ccc}
N_x, & N_y, & N_{xy} \\
M_x^b, & M_y^b, & M_{xy}^b \\
M_x^s, & M_y^s, & M_{xy}^s
\end{array}
\right\}
= \sum_{n=1}^{3} \int_{h_{n-1}}^{h_n} \left(\sigma_x, \sigma_y, \tau_{xy} \right)^{(n)}
\left\{
\begin{array}{c}
1 \\
z \\
f(z)
\end{array}
\right\} dz,
\tag{17a}
$$

$$
\left(S_{xz}^s, S_{yz}^s \right) = \sum_{n=1}^{3} \int_{h_{n-1}}^{h_n} \left(\tau_{xz}, \tau_{yz} \right)^{(n)} g(z) dz.
\tag{17b}
$$

where h_n and h_{n-1} are the top and bottom z-coordinates of the nth layer.

Using Eq. (13) in Eq. (17), the stress resultants of a sandwich plate made up of three layers can be related to the total strains by

$$
\left\{
\begin{array}{c}
N \\
M^b \\
M^s
\end{array}
\right\}
=
\begin{bmatrix}
A & B & B^s \\
B & D & D^s \\
B^s & D^s & H^s
\end{bmatrix}
\left\{
\begin{array}{c}
\varepsilon \\
k^b \\
k^s
\end{array}
\right\}
-
\left\{
\begin{array}{c}
N^T \\
M^{bT} \\
M^{sT}
\end{array}
\right\},
\qquad S = A^s \gamma
\tag{18}
$$

where

$$
N = \left\{ N_x, N_y, N_{xy} \right\}^t, \quad M^b = \left\{ M_x^b, M_y^b, M_{xy}^b \right\}^t, \quad M^s = \left\{ M_x^s, M_y^s, M_{xy}^s \right\}^t,
\tag{19a}
$$

$$
N^T = \left\{ N_x^T, N_y^T, 0 \right\}^t, \quad M^{bT} = \left\{ M_x^{bT}, M_y^{bT}, 0 \right\}^t, \quad M^{sT} = \left\{ M_x^{sT}, M_y^{sT}, 0 \right\}^t,
\tag{19b}
$$

$$
\varepsilon = \left\{ \varepsilon_x^0, \varepsilon_y^0, \gamma_{xy}^0 \right\}^t, \quad k^b = \left\{ k_x^b, k_y^b, k_{xy}^b \right\}^t, \quad k^s = \left\{ k_x^s, k_y^s, k_{xy}^s \right\}^t,
\tag{19c}
$$

$$
A =
\begin{bmatrix}
A_{11} & A_{12} & 0 \\
A_{12} & A_{22} & 0 \\
0 & 0 & A_{66}
\end{bmatrix},
\quad
B =
\begin{bmatrix}
B_{11} & B_{12} & 0 \\
B_{12} & B_{22} & 0 \\
0 & 0 & B_{66}
\end{bmatrix},
\quad
D =
\begin{bmatrix}
D_{11} & D_{12} & 0 \\
D_{12} & D_{22} & 0 \\
0 & 0 & D_{66}
\end{bmatrix},
\tag{19d}
$$

$$
B^s =
\begin{bmatrix}
B_{11}^s & B_{12}^s & 0 \\
B_{12}^s & B_{22}^s & 0 \\
0 & 0 & B_{66}^s
\end{bmatrix},
\quad
D^s =
\begin{bmatrix}
D_{11}^s & D_{12}^s & 0 \\
D_{12}^s & D_{22}^s & 0 \\
0 & 0 & D_{66}^s
\end{bmatrix},
\quad
H^s =
\begin{bmatrix}
H_{11}^s & H_{12}^s & 0 \\
H_{12}^s & H_{22}^s & 0 \\
0 & 0 & H_{66}^s
\end{bmatrix},
\tag{19e}
$$

$$
S = \left\{ S_{yz}^s, S_{xz}^s \right\}^t, \quad \gamma = \left\{ \gamma_{yz}, \gamma_{xz} \right\}^t, \quad A^s =
\begin{bmatrix}
A_{44}^s & 0 \\
0 & A_{55}^s
\end{bmatrix},
\tag{19f}
$$

where A_{ij}, B_{ij}, etc., are the plate stiffness, defined by

$$
\left\{
\begin{array}{cccccc}
A_{11} & B_{11} & D_{11} & B_{11}^s & D_{11}^s & H_{11}^s \\
A_{12} & B_{12} & D_{12} & B_{12}^s & D_{12}^s & H_{12}^s \\
A_{66} & B_{66} & D_{66} & B_{66}^s & D_{66}^s & H_{66}^s
\end{array}
\right\}
= \sum_{n=1}^{3} \int_{h_{n-1}}^{h_n} Q_{11}^{(n)} \left(1, z, z^2, f(z), z\,f(z), f^2(z) \right)
\left\{
\begin{array}{c}
1 \\
\nu^{(n)} \\
\dfrac{1 - \nu^{(n)}}{2}
\end{array}
\right\} dz
\tag{20a}
$$

and

$$
\left(A_{22}, B_{22}, D_{22}, B_{22}^s, D_{22}^s, H_{22}^s \right) = \left(A_{11}, B_{11}, D_{11}, B_{11}^s, D_{11}^s, H_{11}^s \right)
\tag{20b}
$$

$$A_{44}^s = A_{55}^s = \sum_{n=1}^{3} \int_{h_{n-1}}^{h_n} \frac{E(z)}{2(1+\nu)}[g(z)]^2 dz, \tag{20c}$$

The stress and moment resultants, $N_x^T = N_y^T$, $M_x^{bT} = M_y^{bT}$, and $M_x^{sT} = M_y^{sT}$ due to thermal loading are defined by

$$\begin{Bmatrix} N_x^T \\ M_x^{bT} \\ M_x^{sT} \end{Bmatrix} = \sum_{n=1}^{3} \int_{h_{n-1}}^{h_n} \frac{E^{(n)}(z)}{1-\nu} \alpha^{(n)}(z)T \begin{Bmatrix} 1 \\ z \\ f(z) \end{Bmatrix} dz, \tag{21}$$

The stability equations of the plate may be derived by the adjacent equilibrium criterion. Assume that the equilibrium state of the FGM plate under thermal loads is defined in terms of the displacement components (u_0^0, v_0^0, w_b^0, w_s^0). The displacement components of a neighboring stable state differ by (u_0^1, v_0^1, w_b^1, w_s^1) with respect to the equilibrium position. Thus, the total displacements of a neighboring state are

$$u_0 = u_0^0 + u_0^1, \quad v_0 = v_0^0 + v_0^1, \quad w_b = w_b^0 + w_b^1, \quad w_s = w_s^0 + w_s^1 \tag{22}$$

where the superscript 1 refers to the state of stability and the superscript 0 refers to the state of equilibrium conditions.

Substituting Eqs. (12) and (22) into Eq. (16) and integrating by parts and then equating the coefficients of δu_0^1, δv_0^1, δw_b^1 and δw_s^1 to zero, separately, the governing stability equations are obtained for the shear deformation plate theories as

$$\frac{\partial N_x^1}{\partial x} + \frac{\partial N_{xy}^1}{\partial y} = 0$$

$$\frac{\partial N_{xy}^1}{\partial x} + \frac{\partial N_y^1}{\partial y} = 0$$

$$\frac{\partial^2 M_x^{b1}}{\partial x^2} + 2\frac{\partial^2 M_{xy}^{b1}}{\partial x \partial y} + \frac{\partial^2 M_y^{b1}}{\partial y^2} + \overline{N} = 0 \tag{23}$$

$$\frac{\partial^2 M_x^{s1}}{\partial x^2} + 2\frac{\partial^2 M_{xy}^{s1}}{\partial x \partial y} + \frac{\partial^2 M_y^{s1}}{\partial y^2} + \frac{\partial S_{xz}^{s1}}{\partial x} + \frac{\partial S_{yz}^{s1}}{\partial y} + \overline{N} = 0$$

with

$$\overline{N} = \left[N_x^0 \frac{\partial^2 (w_b^1 + w_s^1)}{\partial x^2} + N_y^0 \frac{\partial^2 (w_b^1 + w_s^1)}{\partial y^2} \right] \tag{24}$$

where

$$N_x^0 = N_y^0 = -\sum_{n=1}^{3} \int_{h_{n-1}}^{h_n} \frac{\alpha^{(n)}(z)E^{(n)}(z)T}{1-\nu} dz. \tag{25}$$

For the CPT, the stability equations are reduced to the first three equations of Eq. (23).

3. Thermal buckling solution

Rectangular plates are generally classified in accordance with the type of support used. We are here concerned with the exact solution of Eqs. (23) for a simply supported FGM sandwich plate. The following boundary conditions are imposed for the present four variable refined plate theory at the side edges

$$v_0^1 = w_b^1 = w_s^1 = \frac{\partial w_s^1}{\partial y} = N_x^1 = M_x^{b1} = M_x^{s1} = 0 \qquad \text{at} \qquad x = 0, \ a, \tag{26a}$$

$$u_0^1 = w_b^1 = w_s^1 = \frac{\partial w_s^1}{\partial x} = N_y^1 = M_y^{b1} = M_y^{s1} = 0 \qquad \text{at} \qquad y = 0, \ b. \tag{26b}$$

The following approximate solution is seen to satisfy both the differential equation and the boundary conditions

$$\begin{Bmatrix} u_0^1 \\ v_0^1 \\ w_b^1 \\ w_s^1 \end{Bmatrix} = \sum_{m=1}^{\infty} \sum_{n=1}^{\infty} \begin{Bmatrix} U_{mn}^1 \cos(\lambda x)\sin(\mu y) \\ V_{mn}^1 \sin(\lambda x)\cos(\mu y) \\ W_{bmn}^1 \sin(\lambda x)\sin(\mu y) \\ W_{smn}^1 \sin(\lambda x)\sin(\mu y) \end{Bmatrix} \tag{27}$$

where U_{mn}^1, V_{mn}^1, W_{bmn}^1, and W_{smn}^1 are arbitrary parameters to be determined and $\lambda = m\pi/a$ and $\mu = n\pi/b$. Substituting Eq. (27) into Eq. (23), one obtains

$$[K]\{\Delta\} = 0, \tag{28}$$

where $\{\Delta\}$ denotes the column

$$\{\Delta\} = \left\{ U_{mn}^1, V_{mn}^1, W_{bmn}^1, W_{smn}^1 \right\}^t \tag{29}$$

and $[K]$ is the symmetric matrix given by

$$[K] = \begin{bmatrix} a_{11} & a_{12} & a_{13} & a_{14} \\ a_{12} & a_{22} & a_{23} & a_{24} \\ a_{13} & a_{23} & a_{33} & a_{34} \\ a_{14} & a_{24} & a_{34} & a_{44} \end{bmatrix}, \tag{30}$$

in which

$$\begin{aligned} a_{11} &= -\left[2\lambda^2 + (1-v)\mu^2\right]\overline{A} \\ a_{12} &= -(1+v)\lambda\,\mu\,\overline{A} \\ a_{13} &= 2\lambda(\lambda^2 + \mu^2)\overline{B} \\ a_{14} &= 2\lambda(\lambda^2 + \mu^2)\overline{B}^s \\ a_{22} &= -\left[(1-v)\lambda^2 + 2\mu^2\right]\overline{A} \\ a_{23} &= 2\mu(\lambda^2 + \mu^2)\overline{B} \end{aligned} \tag{31-1}$$

$$a_{24} = 2\mu\left(\lambda^2 + \mu^2\right)\overline{B^s}$$

$$a_{33} = -2\left(\lambda^2 + \mu^2\right)^2\overline{D} - 2\overline{N_x^0}\lambda^2 - 2\overline{N_y^0}\mu^2$$

$$a_{34} = -2\left(\lambda^2 + \mu^2\right)^2\overline{D^s} - 2\overline{N_x^0}\lambda^2 - 2\overline{N_y^0}\mu^2$$

$$a_{44} = -2\left(\lambda^2 + \mu^2\right)^2\overline{H^s} - 2\overline{J}\left(\lambda^2 + \mu^2\right) - 2\lambda^2\,\overline{N_x^0} - 2\mu^2\,\overline{N_y^0}$$

(31-2)

where

$$\mathfrak{R}_{11} = \mathfrak{R}_{22} = \overline{\mathfrak{R}}, \quad \mathfrak{R}_{12} = \nu\,\overline{\mathfrak{R}}, \quad \mathfrak{R}_{66} = \frac{1-\nu}{2}\,\overline{\mathfrak{R}}, \quad A_{44}^s = A_{55}^s = \overline{J} \quad \left(\mathfrak{R} = A, B, B^s, D, D^s, H^s\right) \quad (32)$$

In the following, the solution of the equation $|K| = 0$ for different types of thermal loading conditions is presented. The plate is assumed simply supported in bending and rigidly fixed in extension. The temperature change is varied only through-the-thickness as the following.

3.1 Buckling of FGM plates under uniform temperature rise

The plate initial temperature is assumed to be T_i. The temperature is uniformly raised to a final value T_f in which the plate buckles. The temperature change is $\Delta T = T_f - T_i$. By solving the determinant

$$\begin{vmatrix} a_{11} & a_{12} & a_{13} & a_{14} \\ a_{12} & a_{22} & a_{23} & a_{24} \\ a_{13} & a_{23} & a_{33} & a_{34} \\ a_{14} & a_{24} & a_{34} & a_{44} \end{vmatrix} = 0, \tag{33}$$

one can easily obtain the critical buckling temperature change ΔT_{cr} as

$$\Delta T_{cr} = \frac{\Pi^2\left[\left(\overline{AD} - \overline{B^2}\right)\overline{H_s} - \overline{B_s^2}\,\overline{D} - \overline{A}\,\overline{D_s^2} + 2\overline{BD_sB_s}\right] + a^2b^2\,\Pi\left(\overline{AD} - \overline{B^2}\right)\overline{J}}{a^2b^2\,\overline{\beta_1}\left[\Pi\left(\left(\overline{H_s} + \overline{D} - 2\overline{D_s}\right)\overline{A} - \left(\overline{B_s} - \overline{B}\right)^2\right) + a^2b^2\,\overline{AJ}\right]} \tag{34}$$

where

$$\Pi = \left(a^2 + b^2\right)\pi^2, \quad \overline{\beta_1} = \sum_{n=1}^{3}\int_{h_{n-1}}^{h_n}\frac{\alpha^{(n)}(z)E^{(n)}(z)}{1-\nu}\,dz. \tag{35}$$

3.2 Buckling of FGM plates subjected to graded temperature change across the thickness

We assume that the temperature of the top surface is T_t and the temperature varies from T_t, according to the power law variation through-the-thickness, to the bottom surface temperature T_b in which the plate buckles. In this case, the temperature through-the-thickness is given by

$$T(z) = \Delta T\left(\frac{z}{h} + \frac{1}{2}\right)^\gamma + T_t, \tag{36}$$

where the buckling temperature difference $\Delta T = T_b - T_t$ and γ is the temperature exponent $(0 < \gamma <$

∞). Note that the value of γ equal to unity represents a linear temperature change across the thickness. While the value of γ excluding unity represents a non-linear temperature change through-the-thickness.

Similar to the previous loading case, the critical buckling temperature change ΔT_{cr} can be deduced, for the present four variable refined plate theory, as

$$\Delta T_{cr} = \frac{\Pi^2\left[\left(\overline{AD}-\overline{B}^2\right)\overline{H_s}-\overline{B_s^2}\overline{D}-\overline{A}\overline{D_s^2}+2\overline{BD_sB_s}\right]+a^2b^2\,\Pi\left(\overline{AD}-\overline{B}^2\right)\overline{J}}{a^2b^2\overline{\beta_2}\left[\Pi\left(\left(\overline{H_s}+\overline{D}-2\overline{D_s}\right)\overline{A}-\left(\overline{B_s}-\overline{B}\right)^2\right)+a^2b^2\,\overline{AJ}\right]}-\frac{T_t\overline{\beta_1}}{\overline{\beta_2}} \qquad (37)$$

where

$$\overline{\beta_2} = \sum_{n=1}^{3}\int_{h_{n-1}}^{h_n}\frac{\alpha^{(n)}(z)E^{(n)}(z)}{1-\nu}\left(\frac{z}{h}+\frac{1}{2}\right)^{\gamma}dz. \qquad (38)$$

4. Numerical results

4.1 Analytical model of bridge pier

To illustrate the proposed approach, a ceramic-metal functionally graded sandwich plate is considered. The combination of materials consists of Titanium and Zirconia. The Young's modulus and the coefficient of thermal expansion for Titanium and Zirconia are given in Table 1.

The general approach outlined in the previous sections for the thermal buckling analysis of the FGM symmetric sandwich plates under uniform, linear and non-linear temperature rises through-the-thickness is illustrated in this section using the four variable refined plate theory.

The shear correction factor for FSDPT is set equal to $5/6$. For the linear and non-linear temperature rises through-the-thickness, $T_t = 25°C$.

Table 1 Material properties used in the FG sandwich plate

Properties	Metal: Ti–6A1–4V	Ceramic: ZrO_2
E (GPa)	66.2	244.27
V	0.3	0.3
α (10^{-6}/K)	10.3	12.766

Table 2 Minimum critical temperature parameter αT_{cr} of the simply supported isotropic plate ($a/b = 1$, $\alpha_0 = 1.0 \times 10^{-6}/K$, $E = 1.0 \times 10^{-6}\,N/m^2$, $v = 0.3$)

a/h	Present theory	Matsunaga (2005)
10	0.1198×10^{-1}	0.1183×10^{-1}
20	0.3119×10^{-2}	0.3109×10^{-2}
100	0.1265×10^{-3}	0.1264×10^{-3}

    In order to validate the accuracy of the present formulations, a comparison has been carried out
with the results obtained by Matsunaga (2005) for homogeneous isotropic plates under uniform
temperature rise. The critical buckling temperature difference has been listed in Table 2. As this
table shows, the present results have a good agreement with those reported in References
(Matsunaga 2005).
    To verify also the accuracy of the present new hyperbolic displacement model (with four
unknown functions), comparisons are made between the thermal buckling results obtained from
the present new hyperbolic displacement model and those obtained by other higher order theories
(with five unknown functions). For a homogeneous isotropic plate $k = 0$, $E(z) = E_0$, $\alpha(z) = \alpha_0$, $v = 0.3$. Critical buckling temperature change ($10^3 a_0 \Delta T_{cr}$) for different values of the side-to-thickness
ratio a/h and aspect ratio b/a of a homogeneous plate is illustrated in Table 3. With the increase of
the side-to-thickness ratio a/h, severe decrement for critical buckling temperature can be clearly
observed. Also, it can be observed that the critical buckling temperature for the homogeneous plate
decreases gradually as the plate aspect ratio b/a increases. The difference between the shear
deformation plate theories and the CPT decreases as the ratios a/h or b/a increase because the
plate becomes thin or long.

Table 3 Critical buckling temperature ($10^3 a_0 \Delta T_{cr}$) of a homogeneous isotropic plate under uniform temperature
        rise

b/a	Theory	$a/h = 5$	$a/h = 10$	$a/h = 15$	$a/h = 25$	$a/h = 50$
	Present	81.15170	27.73347	13.23144	4.94979	1.25825
	SSDPT	81.18685	27.73638	13.23205	4.94987	1.25825
0.5	TSDPT	81.09991	27.73011	13.23079	4.94970	1.25824
	FSDPT	80.90487	27.72437	13.23021	4.94968	1.25824
	CPT	126.53339	31.63335	14.05927	5.06134	1.26533
	Present	41.32613	11.97877	5.48633	2.00644	0.50500
	SSDPT	41.33313	11.97927	5.48643	2.00646	0.50500
1	TSDPT	41.31747	11.97825	5.48623	2.00643	0.50499
	FSDPT	41.29710	11.97782	5.48619	2.00643	0.50499
	CPT	50.61336	12.65334	5.62371	2.02453	0.50613
	Present	27.73347	7.63938	3.46065	1.25824	0.31589
	SSDPT	27.73638	7.63958	3.46069	1.25825	0.31589
2	TSDPT	27.73011	7.63918	3.46061	1.25824	0.31589
	FSDPT	27.72437	7.63907	3.46060	1.25824	0.31589
	CPT	31.63335	7.90834	3.51482	1.26533	0.31633
	Present	23.56145	6.39248	2.88674	1.04785	0.26288
	SSDPT	23.56351	6.39261	2.88676	1.04785	0.26288
5	TSDPT	23.55914	6.39233	2.88671	1.04784	0.26288
	FSDPT	23.55569	6.39227	2.88670	1.04784	0.26288
	CPT	26.31895	6.57974	2.92433	1.05276	0.26319

Table 4 Critical buckling temperature ΔT_{cr} of FGM sandwich square plates under uniform temperature rise versus volume fraction index k and t_C/h ($a/h = 5$)

t_C/h	Theory	k						
		0	0.2	0.5	1	2	5	10
0	Present	3.23720	3.07138	2.87207	2.68975	2.63325	2.93978	3.30959
	SSDPT	3.23775	3.07197	2.87277	2.69065	2.63460	2.94205	3.31226
	TSDPT	3.23652	3.07042	2.87074	2.68781	2.63018	2.93446	3.30340
	FSDPT	3.23493	3.04858	2.83507	2.64222	2.57355	2.86226	3.23289
	CPT	3.96470	3.66606	3.34559	3.06734	2.96200	3.32950	3.82441
0.2	Present	3.23720	3.05543	2.83135	2.59388	2.39856	2.35252	2.42641
	SSDPT	3.23775	3.05598	2.83194	2.59458	2.39953	2.35401	2.42827
	TSDPT	3.23652	3.05461	2.83030	2.59241	2.39637	2.34898	2.42195
	FSDPT	3.23493	3.03394	2.79675	2.55053	2.34734	2.28926	2.35538
	CPT	3.96470	3.64978	3.30066	2.95538	2.68016	2.59922	2.68195
0.4	Present	3.23720	3.05915	2.84285	2.60512	2.37406	2.19921	2.17624
	SSDPT	3.23775	3.05956	2.84318	2.60545	2.37450	2.19992	2.17714
	TSDPT	3.23652	3.05867	2.84246	2.60462	2.37320	2.19763	2.17417
	FSDPT	3.23493	3.04171	2.81495	2.57038	2.33409	2.15296	2.12571
	CPT	3.96470	3.66567	3.33354	2.99117	2.67295	2.43609	2.39804
0.5	Present	3.23720	3.06980	2.86974	2.64965	2.42885	2.23972	2.17737
	SSDPT	3.23775	3.07014	2.86992	2.64976	2.42900	2.24005	2.17784
	TSDPT	3.23652	3.06952	2.86972	2.64970	2.42873	2.23910	2.17640
	FSDPT	3.23493	3.05527	2.84659	2.62069	2.39542	2.20130	2.13606
	CPT	3.96470	3.68764	3.38155	3.06366	2.75801	2.50252	2.41816
0.6	Present	3.23720	3.08713	2.91139	2.71917	2.52309	2.34313	2.27452
	SSDPT	3.23775	3.08741	2.91146	2.71909	2.52297	2.34310	2.27458
	TSDPT	3.23652	3.08699	2.91168	2.71971	2.52367	2.34345	2.27461
	FSDPT	3.23493	3.07586	2.89364	2.69680	2.49698	2.31286	2.24190
	CPT	3.96470	3.71993	3.45164	3.17226	2.89771	2.65182	2.55878
0.8	Present	3.23720	3.14445	3.04101	2.93052	2.81681	2.74134	2.65659
	SSDPT	3.23775	3.14474	3.04107	2.93038	2.81650	2.74092	2.65609
	TSDPT	3.23652	3.14431	3.04137	2.93131	2.81794	2.74272	2.65798
	FSDPT	3.23493	3.13952	3.03406	2.92193	2.80661	2.72895	2.64315
	CPT	3.96470	3.81800	3.66058	3.49712	3.33246	3.21552	3.10423
1	Present	3.23720	3.23720	3.23720	3.23720	3.23720	3.23720	3.23720
	SSDPT	3.23775	3.23775	3.23775	3.23775	3.23775	3.23775	3.23775
	TSDPT	3.23652	3.23652	3.23652	3.23652	3.23652	3.23652	3.23652
	FSDPT	3.23493	3.23493	3.23493	3.23493	3.23493	3.23493	3.23493
	CPT	3.96470	3.96470	3.96470	3.96470	3.96470	3.96470	3.96470

F.Z. Kettaf, M.S.A. Houari, M. Benguediab and A. Tounsi

Table 5 Critical buckling temperature T_{cr} of FGM sandwich square plates under linear temperature rise versus volume fraction index k and t_C/h ($a/h = 5$)

t_C/h	Theory	k						
		0	0.2	0.5	1	2	5	10
0	Present	6.42441	6.09275	5.69414	5.32949	5.21651	5.82957	6.56918
	SSDPT	6.42550	6.09396	5.69554	5.33130	5.21920	5.83411	6.57458
	TSDPT	6.42305	6.09084	5.69148	5.32562	5.21036	5.81891	6.55680
	FSDPT	6.41986	6.04716	5.62014	5.23443	5.09711	5.67452	6.41578
	CPT	7.87940	7.28211	6.64118	6.08468	5.87400	6.60901	7.59882
0.2	Present	6.42441	6.06087	5.61271	5.13775	4.74712	4.65504	4.80264
	SSDPT	6.42550	6.06197	5.61388	5.13917	4.74907	4.65803	4.80632
	TSDPT	6.42305	6.05922	5.61059	5.13482	4.74275	4.64797	4.79372
	FSDPT	6.41986	6.01789	5.54350	5.05105	4.64468	4.52851	4.66058
	CPT	7.87940	7.24955	6.55131	5.86076	5.31032	5.14843	5.31369
0.4	Present	6.42441	6.06830	5.63571	5.16024	4.69812	4.34842	4.26735
	SSDPT	6.42550	6.06913	5.63636	5.16089	4.69900	4.34984	4.24818
	TSDPT	6.42305	6.06734	5.63491	5.15923	4.69640	4.34526	4.26325
	FSDPT	6.41986	6.03341	5.57990	5.09075	4.61818	4.25591	4.16712
	CPT	7.87940	7.28133	6.61708	5.93233	5.29588	4.82217	4.70737
0.5	Present	6.42441	6.08961	5.68948	5.24929	4.80770	4.42943	4.30474
	SSDPT	6.42550	6.09029	5.68986	5.24952	4.80800	4.43011	4.30569
	TSDPT	6.42305	6.08903	5.68943	5.24940	4.80746	4.42821	4.30281
	FSDPT	6.41986	6.06053	5.64319	5.19137	4.74084	4.35259	4.22211
	CPT	7.87940	7.32529	6.71310	6.07732	5.46601	4.95505	4.78633
0.6	Present	6.42441	6.12425	5.77278	5.38833	4.99619	4.63616	4.49905
	SSDPT	6.42550	6.12482	5.77291	5.38818	4.99595	4.63609	4.84881
	TSDPT	6.42305	6.12398	5.77335	5.38942	4.99734	4.63680	4.49922
	FSDPT	6.41986	6.10171	5.73728	5.34361	4.94396	4.57561	4.43382
	CPT	7.87940	7.38985	6.85328	6.29453	5.74542	5.25352	5.06756
0.8	Present	6.42441	6.23889	6.03202	5.81104	5.58362	5.35987	5.26317
	SSDPT	6.42550	6.23949	6.03215	5.81076	5.58301	5.35923	5.26229
	TSDPT	6.42305	6.23862	6.03273	5.81262	5.58589	5.36259	5.26598
	FSDPT	6.41986	6.22905	6.01812	5.79385	5.56322	5.33541	5.23630
	CPT	7.87940	7.58600	7.27115	6.94424	6.61492	6.29563	6.15846
1	Present	6.42441	6.42441	6.42441	6.42441	6.42441	6.42441	6.42441
	SSDPT	6.42550	6.42550	6.42550	6.42550	6.42550	6.42550	6.42550
	TSDPT	6.42305	6.42305	6.42305	6.42305	6.42305	6.42305	6.42305
	FSDPT	6.41986	6.41986	6.41986	6.41986	6.41986	6.41986	6.41986
	CPT	6.42363	6.12545	5.77544	5.39175	4.99944	4.63813	4.49981

Table 6 Critical buckling temperature T_{cr} of FGM sandwich square plates under non-linear temperature rise versus volume fraction index k and t_C/h ($a/h = 5$ and $\gamma = 5$)

t_C/h	Theory	k						
		0	0.2	0.5	1	2	5	10
0	Present	19.27322	20.57122	21.62347	22.42701	23.05643	23.75304	24.05661
	SSDPT	19.27655	20.57531	21.62882	22.43468	23.06838	23.77163	24.07624
	TSDPT	19.26915	20.56479	21.61337	22.41074	23.02926	23.70963	24.01127
	FSDPT	19.25957	20.41729	21.34246	22.02700	22.52869	23.12129	23.49484
	CPT	23.63820	24.58692	25.21986	25.60494	25.96247	26.92893	27.82720
0.2	Present	19.27322	20.43016	21.34626	21.99533	22.37338	22.64929	22.85562
	SSDPT	19.27655	20.43388	21.35077	22.00145	22.38259	22.66392	22.87344
	TSDPT	19.26915	20.42463	21.33822	21.98279	22.35275	22.61489	22.81317
	FSDPT	19.25957	20.28528	21.08307	21.62417	21.89055	22.03367	22.17958
	CPT	23.63820	24.43703	24.91598	25.09061	25.02775	25.04991	25.28770
0.4	Present	19.27322	20.24553	21.00745	21.54152	21.81937	21.87237	21.87534
	SSDPT	19.27655	20.24830	21.00993	21.54429	21.82352	21.87961	21.88463
	TSDPT	19.26915	20.24234	21.00447	21.53734	21.81141	21.85652	21.85429
	FSDPT	19.25957	20.12913	20.79943	21.25144	21.44811	21.40709	21.36153
	CPT	23.63820	24.29255	24.66557	24.76464	24.59556	24.25535	24.13098
0.5	Present	19.27322	20.13209	20.80394	21.28287	21.54783	21.60059	21.57856
	SSDPT	19.27655	20.13435	20.80531	21.28380	21.54921	21.60389	21.58333
	TSDPT	19.26915	20.13019	20.80375	21.28330	21.54679	21.59462	21.56887
	FSDPT	19.25957	20.03597	20.63466	21.04804	21.24818	21.22586	21.16437
	CPT	23.63820	24.21722	24.54686	24.64006	24.49836	24.16380	23.99263
0.6	Present	19.27322	20.00176	20.57076	20.98623	21.23955	21.32555	21.31715
	SSDPT	19.27655	20.00362	20.57125	20.98565	21.23856	21.32526	21.31771
	TSDPT	19.26915	20.00087	20.57280	20.99045	21.24446	21.32848	21.31794
	FSDPT	19.25957	19.92815	20.44424	20.81202	21.01752	21.04701	21.00808
	CPT	23.63820	24.13520	24.42100	24.51562	24.42463	24.16529	24.01085
0.8	Present	19.27322	19.68210	19.99784	20.23872	20.41383	20.52740	20.55953
	SSDPT	19.27655	19.68400	19.99828	20.23774	20.41159	20.52420	20.55608
	TSDPT	19.26915	19.68124	20.00022	20.24422	20.42213	20.53780	20.57050
	FSDPT	19.25957	19.65105	19.95177	20.17887	20.33926	20.43371	20.45455
	CPT	23.63820	23.93190	24.10594	24.18546	24.18431	24.11121	24.05679
1	Present	19.27322	19.27322	19.27322	19.27322	19.27322	19.27322	19.27322
	SSDPT	19.27655	19.27655	19.27655	19.27655	19.27655	19.27655	19.27655
	TSDPT	19.26915	19.26915	19.26915	19.26915	19.26915	19.26915	19.26915
	FSDPT	19.25957	19.25957	19.25957	19.25957	19.25957	19.25957	19.25957
	CPT	23.63820	23.63820	23.63820	23.63820	23.63820	23.63820	23.63820

Tables 4-6 show the critical buckling temperature difference ($T_{cr} = 10^{-3}\Delta T_{cr}$) for FGM sandwich plates for the uniform, linear and nonlinear cases of temperature distribution through the thickness, respectively. The comparison between the present new hyperbolic displacement model and different higher- and first-order shear deformation theories and classical plate theory is established. As observed in Tables 4-6, there is a very good agreement between the present model (with four unknown functions) and other higher-order plate theories (with five unknown functions). Tables 4-6 show also the influence of the layer thickness of the core t_C (ceramic layer) on the thermal buckling behavior for the FGM sandwich plates. As can be seen from Tables 4 and 5, the thermal buckling temperatures decrease with the increase in volume fraction index k. Thus, the increase in thermal buckling temperature of an FGM sandwich plate could be attributed to the ceramic property. Indeed, this observation is also confirmed when a small volume fraction index is considered ($k \leq 2$) for all values of t_C. A small volume fraction index k indicates that the ceramic is the dominant constituent in FGM sandwich plates. However, Table 6 indicates that the thermal buckling temperatures increase with the increase in volume fraction index k when the plate is under non-linear temperature rise with $\gamma = 5$. It can be observed that the thermal buckling temperature decreases with the increasing thickness of the thickness of the core layer (t_C) for all considered volume fraction index.

Fig. 3 shows the effect of the volume fraction index k on the critical buckling temperature T_{cr} for different thickness of the core t_C of FGM sandwich plates under uniform, linear and non-linear temperature change through-the-thickness using the present new hyperbolic displacement model. It is clear that the critical buckling temperature T_{cr} for the plates under a non-linear temperature change is higher than that for the plates under uniform temperature change. While T_{cr} for the plates under linear temperature change is intermediate to the two previous thermal loading cases. It is further observed that, for the plate without core ($t_C = 0$), the critical buckling T_{cr} decreases rabidly to reach minimum values and then increases gradually as the volume fraction index k increases as shown in Fig. 3(a). However, for the FGM sandwich plates with a ceramic core, T_{cr} decreases smoothly as k increases (see Figs. 3(b), (c) and (d)).


(a)
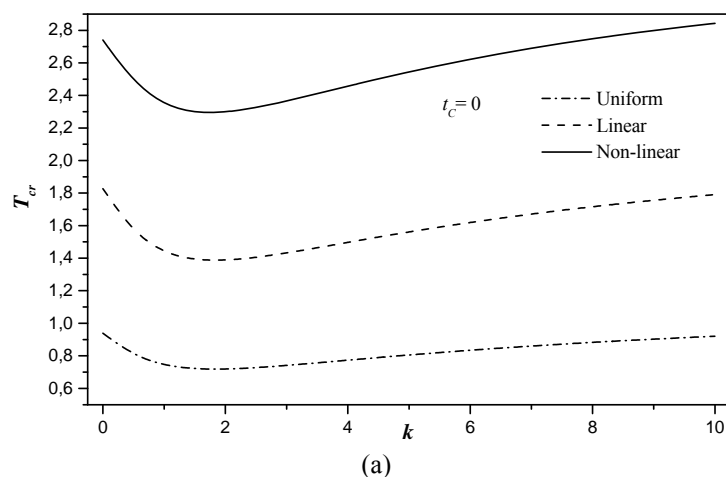
Fig. 3 Critical buckling temperature difference T_{cr} versus the power-law index k for various types of FGM sandwich square plates with $a/h = 10$: (a) $t_C = 0$, (b) $t_C = 0.4$, (c) $t_C = 0.6$, and (d) $t_C = 0.8$. For non-linear temperature $\gamma = 2$
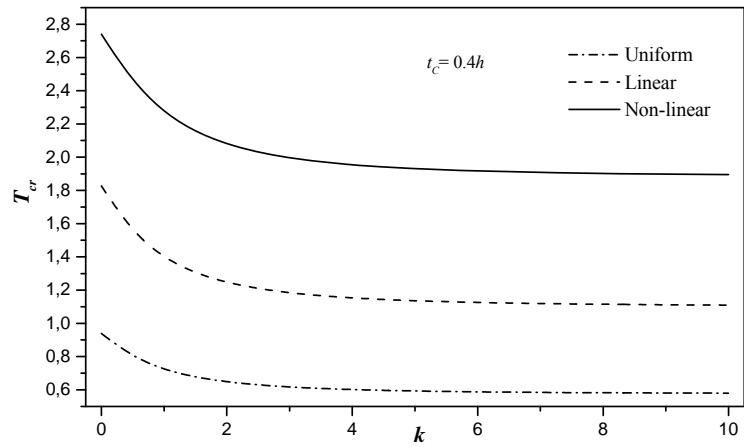
(b)
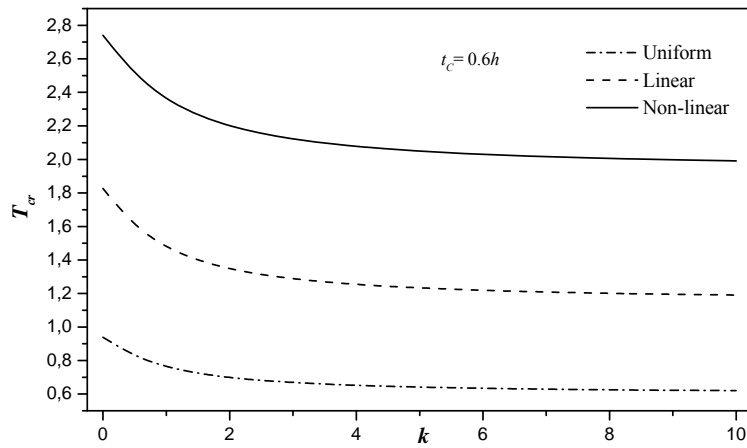
(c)
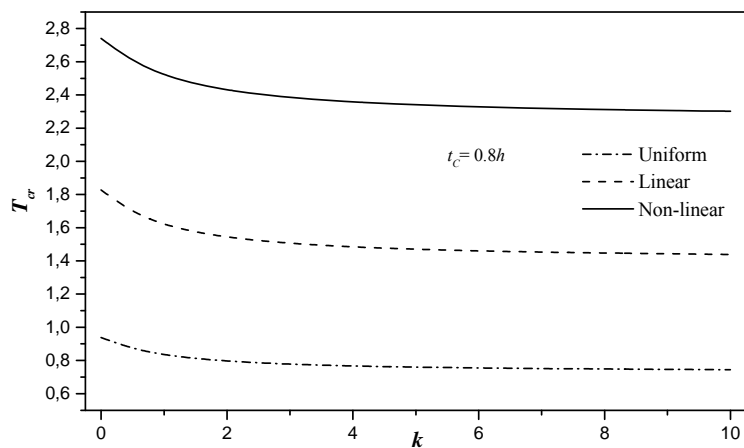
(d)

Fig. 3 Continuous
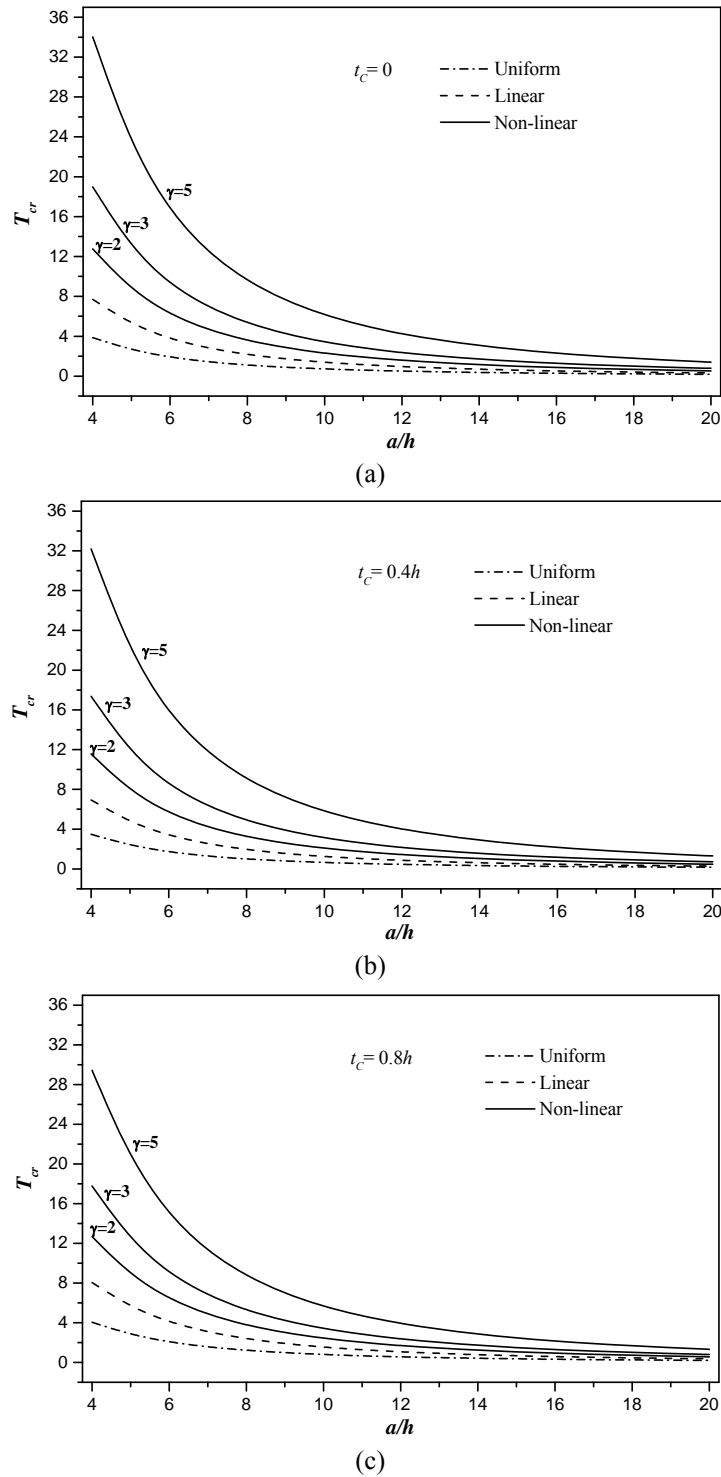
Fig. 4 Critical buckling temperature difference T_{cr} versus the side-to-thickness ratio a/h for various types of FGM sandwich square plates ($k = 2$): (a) $t_C = 0$, (b) $t_C = 0.4$, (c) $t_C = 0.8$

The variation of critical temperatures T_{cr} of FGM sandwich square plates subjected to various thermal loading types is shown in Fig. 4 with respect to the side-to-thickness ratio a/h. It is seen that the critical temperature difference decreases monotonically as the side-to-thickness ratio a/h increases.

Note that the critical temperatures T_{cr} of the FGM plate under uniform temperature rise is smaller than that of the plate under linear temperature rise and the latter is smaller than that of the plate under non-linear temperature rise. Also, it is noticed that T_{cr} increases as the nonlinearity parameter γ increases.

Fig. 5 shows the effects of the aspect ratio b/a on the critical buckling temperature change T_{cr} of FGM sandwich plates under various thermal loading types. It is seen that, regardless of the sandwich plate types, the critical buckling T_{cr} decreases gradually with the increase of the plate aspect ratio b/a wherever the loading type is. It is also noticed from Fig. 5 that the T_{cr} increases with the increase of the non-linearity parameter γ.


(a)

(b)
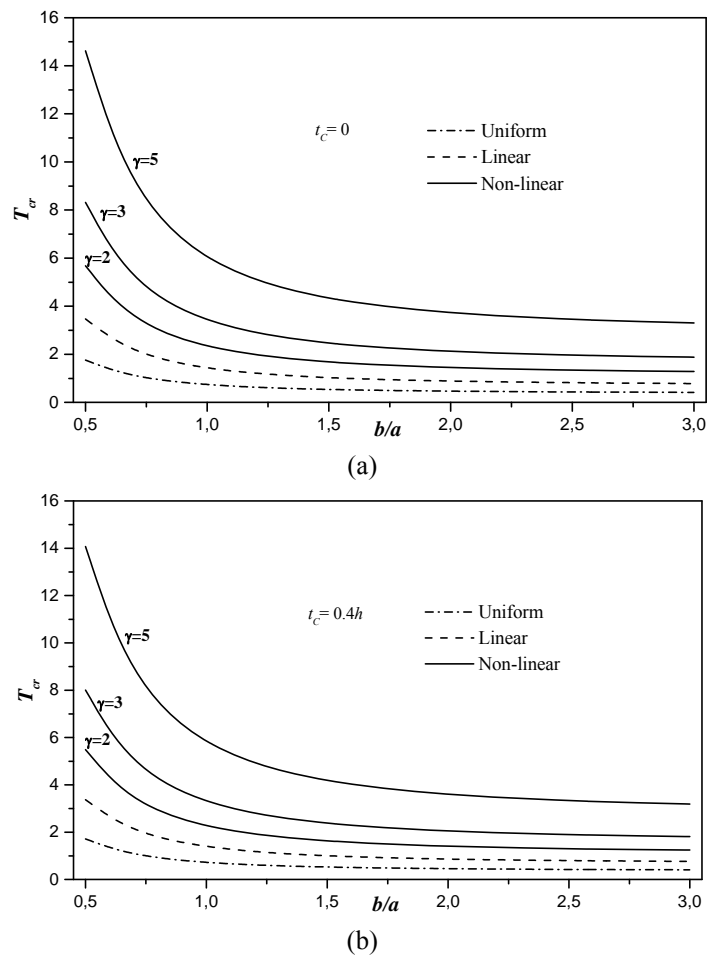
Fig. 5 Critical buckling temperature difference T_{cr} versus the plate aspect ratio b/a for various types of FGM sandwich square plates ($k = 1$, $a/h = 10$): (a) $t_C = 0$, (b) $t_C = 0.4$, (c) $t_C = 0.8$
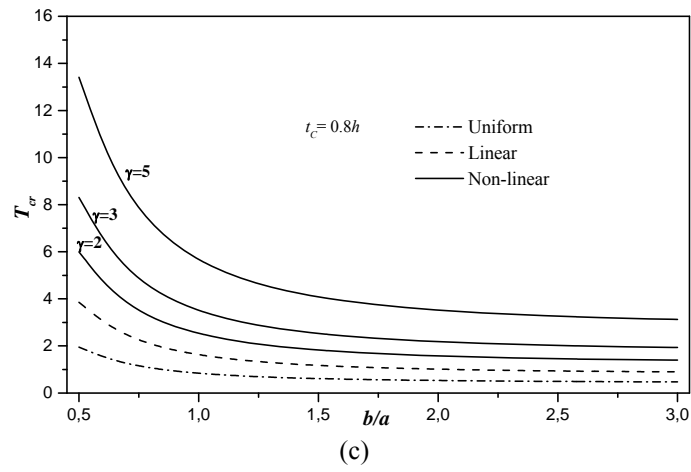
(c)

Fig. 5 Continued
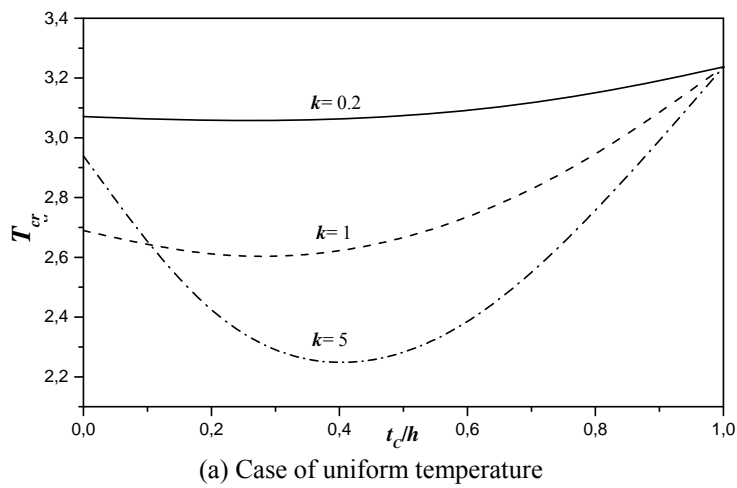
(a) Case of uniform temperature
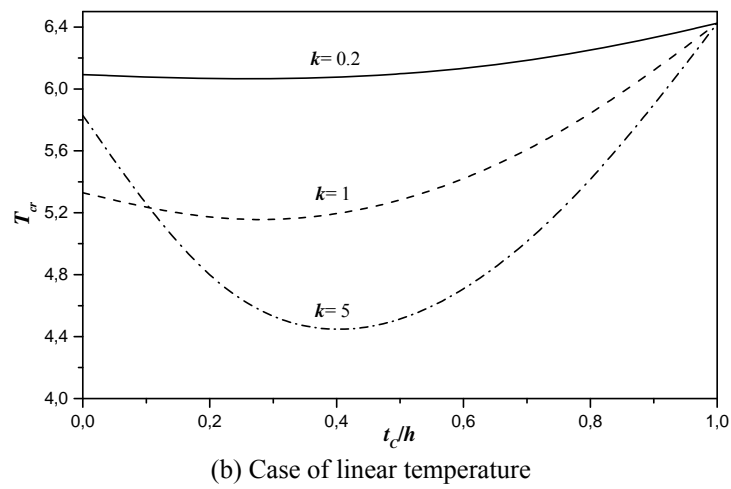

(b) Case of linear temperature

Fig. 6 Critical buckling temperature change T_{cr} of FGM sandwich square plates versus k and t_C/h: (a) uniform temperature; (b) linear temperature; (c) non-linear temperature ($\gamma = 5$)
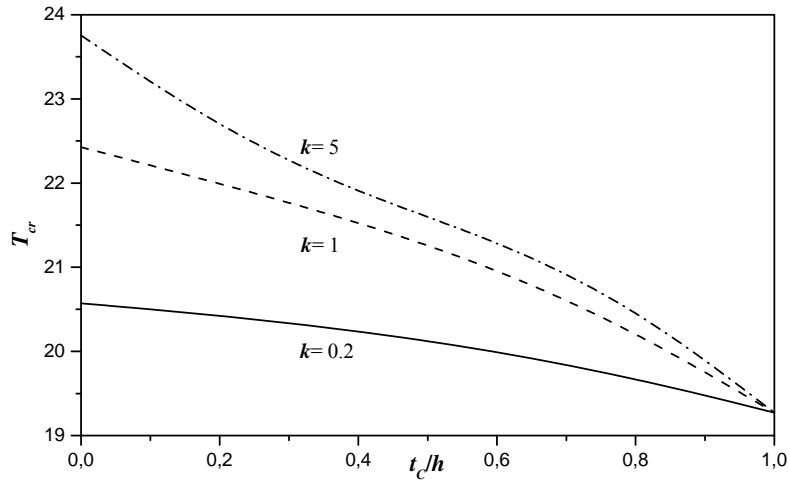
(c) Case of non-linear temperature

Fig. 6 Continued

Fig. 6 shows the influence of layer thickness of the core t_C on the thermal buckling behavior for the FG sandwich plates for the uniform, linear and nonlinear cases of temperature distribution through the thickness, respectively. As can be seen from Figs. 6(a) and (b) (uniform and linear temperature), the thermal buckling temperatures decrease with the increase in volume fraction index. A small volume fraction index k indicates that the ceramic is the dominant constituent in the FGM plate. In addition, it is observed that the thermal buckling temperatures increase for $t_C \geq 0.4$ which means that the ceramic is also the dominant constituent in the FGM plate. Thus, the increase in thermal buckling temperature of an FGM sandwich plate could be attributed to the ceramic property. As expected, the thermal buckling temperature will be maximum for the pure-ceramic plate ($t_C / h = 1$) in the cases of uniform and linear temperature distribution through the thickness of the plate. However, in case of nonlinear temperature distribution (Fig. 6(c)), the thermal buckling temperature will be minimum for the pure-ceramic plate and the thermal buckling temperatures increase with the increase in volume fraction index.

5. Conclusions

The thermal buckling behaviors of functionally graded sandwich plates are described and discussed in this paper using a new hyperbolic displacement model. The number of primary variables in this theory is even less than that of first- and higher-order shear deformation plate theories. The theory gives parabolic distribution of transverse shear strains, and satisfies the zero traction boundary conditions on the surfaces of the plate without using shear correction factors. The material properties of an FGM varies according to a simply power law along the thickness. The buckling analysis of FGM sandwich plates under different types of thermal loadings is presented. In conclusion, it can be said that the proposed new hyperbolic displacement model is accurate and simple in solving the thermal buckling behaviors of FGM sandwich plates.

References

Ameur, M., Tounsi, A., Mechab, I. and Adda Bedia, E.A. (2011), "A new trigonometric shear deformation theory for bending analysis of functionally graded plates resting on elastic foundations", *KSCE J. Civil Eng.*, **15**(8), 1405-1414.

Bouazza, M., Tounsi, A., Adda-Bedia, E.A. and Megueni, A. (2010), "Thermoelastic stability analysis of functionally graded plates: An analytical approach", *Comput. Mater. Sci.*, **49**(4), 865-870.

Bouderba, B., Houari, M.S.A. and Tounsi, A. (2013), "Thermomechanical bending response of FGM thick plates resting on Winkler-Pasternak elastic foundations", *Steel Compos. Struct. Int. J.*, **14**(1), 85-104.

Bourada, M., Tounsi, A., Houari, M.S.A. and Adda Bedia, E.A. (2012), "A new four-variable refined plate theory for thermal buckling analysis of functionally graded sandwich plates", *J. Sandw. Struct. Mater.*, **14**(1), 5-33.

El Meiche, N., Tounsi, A., Ziane, N., Mechab, I. and Adda Bedia, E.A. (2011), "A new hyperbolic shear deformation theory for buckling and vibration of functionally graded sandwich plate", *Int. J. Mech. Sci.*, **53**(4), 237-247.

Fekrar, A., El Meiche, N., Bessaim, A., Tounsi, A. and Adda Bedia, E.A. (2012), "Buckling analysis of functionally graded hybrid composite plates using a new four variable refined plate theory", *Steel Compos. Struct. Int. J.*, **13**(1), 91-107.

Houari, M.S.A, Benyoucef, S., Mechab, I., Tounsi, A. and Adda bedia, E.A. (2011), "Two variable refined plate theory for thermoelastic bending analysis of functionally graded sandwich plates", *J. Therm. Stresses*, **34**(4), 315-334.

Javaheri, R. and Eslami, M.R. (2002a), "Thermal buckling of functionally graded plates", *AIAA J.*, **40**(1), 162-169.

Javaheri, R. and Eslami, M.R. (2002b), "Thermal buckling of functionally graded plates based on higher order theory", *J. Therm. Stresses*, **25**(7), 603-625.

Kiani, Y. and Eslami, M.R. (2012), "Thermal buckling and post-buckling response of imperfect temperature-dependent sandwich FGM plates resting on elastic foundation", *Arch. Appl. Mech.*, **82**(7), 891-905.

Liew, K.M., Yang, J. and Kitipornchai, S. (2004), "Thermal post-buckling of laminated plates comprising functionally graded materials with temperature-dependent properties", *J. Appl. Mech. Trans. ASME.*, **71**(6), 839-850.

Matsunaga, H. (2005), "Thermal buckling of cross-ply laminated composite and sandwich plates according to a global higher-order deformation theory", *Compos. Struct.*, **68**(4), 439-454.

Matsunaga, H. (2009), "Thermal buckling of functionally graded plates according to a 2D higher-order deformation theory", *Compos. Struct.*, **90**(1), 76-86.

Merdaci, S., Tounsi, A., Houari, M.S.A, Mechab, I., Hebali, H. and Benyoucef, S. (2011), "Two new refined shear displacement models for functionally graded sandwich plates", *Arch. Appl. Mech.*, **81**(11), 1507-1522.

Na, K.-S. and Kim, J.-H. (2006), "Three-dimensional thermomechanical buckling analysis for functionally graded composite plates", *Compos. Struct.*, **73**(4), 413-422.

Reddy, J.N. (1984), "A simple higher-order theory for laminated composite plates", *J. Appl. Mech.*, **51**(4), 745-752.

Reddy, J.N. (2000), "Analysis of functionally graded plates", *Int. J. Numer. Methods Eng.*, **47**(1-3), 663-684.

Sallai, B.O., Tounsi, A., Mechab, I., Bachir, B.M., Meradjah, M. and Adda Bedia E.A. (2009), "A theoretical analysis of flexional bending of Al/Al$_2$O$_3$ S-FGM thick beams", *Computat. Mater. Sci.*, **44**(4), 1344-1350.

Samsam Shariat, B.A. and Eslami, M.R. (2005), "Buckling of functionally graded plates under in-plane compressive loading based on the first order plate theory", *Proceeding of the Fifth International Conference on Composite Science and Technology*, Sharjah, UAE, February.

Samsam Shariat, B.A. and Eslami, M.R. (2007), "Buckling of thick functionally graded plates under

mechanical and thermal loads", *Compos. Struct.*, **78**(3), 433-439.

Şimşek, M. (2009), "Static analysis of a functionally graded beam under a uniformly distributed load by Ritz method", *Int. J. Eng. Appl. Sci.*, **1**(3), 1-11.

Wu, L. (2004), "Thermal buckling of a simply supported moderately thick rectangular FGM plate", *Compos. Struct.*, **64**(2), 211-218.

Yaghoobi, H. and Yaghoobi, P. (2013), "Buckling analysis of sandwich plates with FGM face sheets resting on elastic foundation with various boundary conditions: An analytical approach", *Meccanica*, **48**(8), 2019-2035.

Zenkour, A.M. (2005), "A comprehensive analysis of functionally graded sandwich plates: Part 1 – deflection and stresses, Part 2 – buckling and free vibration", *Int. J. Solids Struct.*, **42**(18-19), 5224-5258.

Zenkour, A.M. and Sobhy, M. (2010), "Thermal buckling of various types of FGM sandwich plates", *Compos. Struct.*, **93**(1), 93-102.

CC